



## **Detection of SAR Signature for Rice Crop using SENTINEL 1A data**

**N.S. Sudarmanian and S. Pazhanivelan<sup>1</sup>**

Agro Climate Research Centre, Tamil Nadu Agricultural University, Coimbatore – 641003

<sup>1</sup>Department of Remote Sensing and GIS, Tamil Nadu Agricultural University, Coimbatore – 641003

E-mail: [sudarnsagri@gmail.com](mailto:sudarnsagri@gmail.com)

### **ABSTRACT**

*Rice (*Oryza sativa* L.) is the primary staple food source for more than half of the world's population and has profound influence on the livelihood of farmers. Lowland rice in tropical and subtropical regions can be detected precisely and its crop growth can be tracked effectively through Synthetic Aperture Radar (SAR) imagery, especially where cloud cover restricts the use of optical imagery. This Research was taken to use multi-temporal C-band SAR data from Sentinel 1A, semi-automated processing chains, in-season field monitoring and end-of-season validation points to map rice crops across Tiruchirappalli District. SAR data have a proven ability to detect lowland rice systems (both irrigated and rainfed) through the unique temporal signature of the backscatter coefficient (also termed sigma naught -  $\sigma^0$ ) exhibited by the crop. Temporal signatures were extracted for each monitoring field and used to generate the dB curves for rice fields. This is due to the interaction of microwave radiation with the crop canopy, increasing from the detection of  $\sigma^0$  minimum (field inundation) to the detection of  $\sigma^0$  maximum (around the tillering stage) between acquisitions four and six. The average maximum value of at peak tillering stage was found to be -8.85 with a range of -7.49 to -8.94 in fields across Tiruchirappalli district. The minimum primary variation was found to be 1.5 to 2.1 and the secondary variation was found to be 2.5 to 3.5 corresponding to growth at vegetative and maximum tillering stage. The primary variation corresponds to the growth from seedling to tillering stage where the addition in LAI and biomass and thereby ground coverage is less. However as the growth advances rice has the tendency to put forth more biomass and thereby resulting more dB values with an addition of 2.5 to 3.5. In all the fields the values tend to drop further from flowering to maturity with values found to be reducing from -8.5 to -11.6. Rice crop shows significant temporal behaviour and a large dynamic range (-14.4 to -8.41dB) during its growth period.*

**Keywords:** Rice, Synthetic Aperture Radar (SAR), Sentinel 1A, Backscatter coefficient, Temporal signature

Received 02.01.2019

Revised 20.01.2019

Accepted 09.03. 2019

### **INTRODUCTION**

Rice (*Oryza sativa* L.) is the primary staple food source for more than half of the world's population and has profound influence on the livelihood of farmers. Due to the fact that most rice systems are generally not subject to seasonal rotations (upland rice is one exception but it accounts for a small portion of the total rice area), an accurate rice extent/area map derived from remote sensing data has high value, because it provides an estimation of variations of the total cultivated extent/area, of the different seasonality/crop practices and to assess shortages, due to drought or flood events. Field soil changes and their evolution over time are not random whenever multi-temporal remote sensing data are analysed. With *a priori* knowledge of the crop calendar and land practices, multi-temporal remote sensing data offer valuable information to determine at the earliest stage of the crop season, when and where fields are prepared and irrigated, and later, the phenological crop status such as flowering, tillering, plant senescence and harvesting.

Remote sensing has the scope for cost effective precise estimates of rice area to support, augment, improve or even replace survey and statistical methods [5]. But the technical challenges are many in the development of large scale dynamic remote sensing-based rice crop information systems. Rice cultivation during the monsoon season [7] which has wide cloud cover, wide range of conditions and environments, small land holdings and diverse and mixed cropping systems [16] are the most challenging factors in limiting the use of remote sensing as tool for rice crop monitoring. Synthetic Aperture Radar (SAR) imagery is a promising option to overcome the issue of cloud cover and substantial research evidences

are available on the suitability of SAR for rice crop mapping in the region. Optical images can complement SAR, but they cannot be relied upon as the main information source. The wide distribution of rice as a major food crop across India envisages large coverage to perfectly capture rice area and requires automated less supervised processing. Rice detection algorithms should be general and robust to suit wide range of practices and environments [2] ranging from irrigated to rainfed rice with different maturities [14] and establishment practices, such as direct seeding or transplanting. The complex rice environments require high resolution imageries and high-frequency acquisitions. Recent and planned launches of SAR sensors coupled with state-of-the art automated processing can provide sustainable solutions to this challenge to map and monitor one of the world's most important crop.

### **Synthetic Aperture Radar Data (SAR)**

Multi-temporal X-band SAR Single Look Complex (SLC) data are available from the Italian Space Agency (ASI/e-GEOS) and GISTDA (Geo-informatics and Space Technology Development Agency) for COSMO-SkyMed (CSK) data and from InfoTerra GmbH for TerraSAR-X (TSX) data. In all cases, data can be obtained in HH polarization with consistent incidence angles in each multi-temporal stack, ranging from 39 to 48 degrees across sites. A large incidence angle is preferred, because (i) wind effects on water (in particular, during land preparation prior to transplanting) are significantly decreased, (ii) the dynamic of the radar backscatter is larger and (iii) the spatial resolution is higher. CSK data are available from four X-band HH-SAR satellites with a 3.12-cm wavelength and a 16-day revisit period for the same satellite with the same observation angle. TSX is provided by one X-band HH SAR satellite with a 3.11-cm wavelength and 11-day revisit period with the same observation angle at Strip map mode (3 m resolution) with a footprint of 30 × 50 km and Scan SAR mode (10 m resolution) with a footprint of 100 × 150 km [18]. With the latest launches, Sentinel 1A and 1B data is available from European Space Agency (ESA) at C band with spatial resolution of 5m and 20m with a temporal resolution of 12 days individually and 6 days in combination.

In recent times a rule-based classification approach and parameter selection approach, in which the rules and parameters are derived from agronomic knowledge of the rice crop and its management, have been developed based on the knowledge of temporal development of rice crop under different conditions and its relation to backscatter to demonstrate SAR-based operational mapping of rice crops across a diverse range of environments with the increasing availability of multi-temporal SAR data [15].

SAR data have a proven ability to detect lowland rice systems (both irrigated and rainfed) through the unique temporal signature of the backscatter coefficient (also termed sigma naught or  $\sigma^{\circ}$ ) exhibited by the crop. In the past years, a large number of publications have been dedicated to better understanding this relationship and applying it to rice detection and rice monitoring [10, 11, 19, 3]. In summary, these studies have shown that lower frequencies (L- and C- band) penetrate deeper into the rice plant than higher frequencies, while only higher frequencies (X-band) interact with grain water content and grain weight sufficiently to show a dual-peak signal in  $\sigma^{\circ}$  during the rice season [8, 19, 17]. Further, short wavelengths (X-, Ka-, Ku-band), especially at large incident angles, are sensitive enough to detect even very small rice seedlings just after transplanting. The correlation between  $\sigma^{\circ}$  and rice biophysical parameters shows that lower frequencies are more closely related to total fresh weight, leaf area index (LAI) and plant height than other parameters [9].

Although  $\sigma^{\circ}$  from X-band is poorly correlated with LAI, it is best correlated with panicle biomass indicating the suitability for a direct assessment of rice grain yield [9, 10]. On the other hand,  $\sigma^{\circ}$  derived from C-band can provide information on par with the normalized difference vegetation index (NDVI) [8]. For X-band, the HH/VV polarization ratio continuously changes as a function of phenology during the vegetative and reproductive stages [12]. For X-band, the HH-VV phase difference is sensitive to early rice plant emergence. Moreover, the use of four polarimetric features derived from coherence coplanar dual-polarization X-band enables the estimation of five phenological stages from a single date scene [9-13].

It is clear from the literature that well-understood relationships exist between rice crop characteristics and backscatter coefficients from different wavelengths, and these relationships have been used to derive different types of algorithms for estimating rice crop characteristics from SAR data. Another approach for sparse time series is to extract temporal features from the data and relate those to the known temporal dynamics of the rice crop and use that knowledge to classify areas as rice or non-rice [6]. All of these approaches have been demonstrated successfully in the literature. Supervised classifiers rely on a substantial set of good-quality training data to ensure a good classification, and there is a risk of over-fitting the classification.

For this reason, a rule-based classification approach has been developed for rice area mapping that is based on a small number of rules and parameters that can be quickly fine-tuned from site to site and season to season. Conceptually, the classification approach is based on rules that are agronomically

meaningful hence easily understood and easily fine-tuned based on the local knowledge of the rice-growing environment and the key rice-growing stages.

### ***Rice Growing Stages and Key Characteristics for SAR Based Detection***

Rice in subtropical India is mainly cultivated in irrigated or lowland semidry conditions. Rice varieties range in duration from 90 to more than 150 days and with three main crop stages *viz.*, vegetative (from germination to panicle initiation, from 45 to 100 days), reproductive (from panicle initiation to flowering, around 35 days) and maturity stages (from flowering to mature grain, around 30 days). The following aspects contribute to the change in space occupied by the rice plants within a three-dimensional space: (1) appearances and growth of leaves from the main stem (culm) and tillers; (2) stem development and elongation; (3) tillering, defined as the production of stems from rice plants; (4) leaf senescence; and (5) panicle and grain development. Prior to transplanting, the rice field is flooded with water at depth ranging from 2 to 15cm [11]. The deliberate agronomic flooding is a key element of most remote-sensing rice detection algorithms [2].

## **MATERIALS AND METHODS**

The Tiruchirappalli district of Tamil Nadu extends over an area of 4,40,383 hectares. Geographically it lies between 78° 10' to 79° 5' East longitudes and 10°15' to 11°2' North latitudes with an altitude of 90 m.

### ***Basic Processing of SAR Data for Multi-Temporal Analysis***

A fully automated processing chain was developed to convert the multi-temporal space-borne SAR data into terrain-geocoded  $\sigma^{\circ}$  values. The processing chain is a module within the MAPscape-RICE software [6]. The basic processing chain included strip mosaicking, coregistration of Images acquired with the same observation geometry and mode and, Time-series speckle filtering to balance differences in reflectivity between images at different times [4] and terrain geocoding, radiometric calibration and normalization. Further Anisotropic non-linear diffusion (ANLD) filtering was done to smoothen homogeneous targets, while enhancing the difference between neighbouring areas. The filter uses the diffusion equation, in which the diffusion coefficient, instead of being a constant scalar, is a function of image position and assumes a tensor value [1].

This multi-temporal stack was analyzed using a rule-based classifier to detect rice areas. The rules for the classifier were based on a small number of parameters that must be selected by the operator or user. Temporal feature descriptors were derived from temporal signatures in the monitored fields and used to guide the user in setting these parameters for each site. It is clear that there must always be a degree of user expertise in the setting of the parameters, relying on expert local knowledge or other sources of information to further guide the parameter values. Finally, the accuracy of the rice area maps was assessed against field data.

## **RESULT AND DISCUSSION**

### ***Multi-Temporal $\sigma^{\circ}$ Rule-Based Rice Detection***

The multi-temporal stack of terrain-geocoded  $\sigma^{\circ}$  images of Sentinel 1A acquired from August, 2015 to January, 2016 was input to a rule-based rice detection algorithm in MAPscape-RICE. The temporal evolution of  $\sigma^{\circ}$  is analyzed from an agronomic perspective, which also requires a priori knowledge of rice maturity, calendar and duration and crop practices from field information and knowledge of the study location. The temporal signature is frequency and polarization dependent and also depends on the crop establishment method and, to some extent, on crop maturity. This implies that general rules can be applied to detect rice, but that the parameters for these rules may need to be adapted according to the agro-ecological zone, crop practices and rice calendar.

A dB stack was generated using ten sets of Sentinel-1A data acquired after basic processing *viz.*, orbital and radiometric correction, geo-coding, mosaicing and Speckle filtering. Temporal signatures were extracted for each monitoring field and used to generate the dB curves for rice fields. Fig. 1 shows the temporal signature for selected representative pixels to visualize the resulting rule based classification. A detailed analysis of temporal signatures of rice showed a minimum at agronomic flooding and a peak at maximum tillering stage (Fig. 2&3). At agronomic flooding, minimum dB value from -14.36 to -11.992 was recorded with an average of -13.35. The average maximum value at peak at tillering stage was found to be -8.85 with a range of -7.49 to -8.94 fields across Tiruchirappalli district (Table. 1). The minimum primary variation was found to be 1.5 to 2.1 and the secondary variation was found to be 2.5 to 3.5 corresponding to growth at vegetative and maximum tillering stage. The primary variation corresponds to the growth from seedling to tillering stage where the addition in LAI and biomass and thereby ground coverage is less. However as the growth advances rice has the tendency to putforth more biomass and thereby resulting more dB values with an addition of 2,5 to 3.5. In all the fields the values tend to drop further from flowering to maturity with values found to be reducing from -8.5 to -11.6 (Table. 2). Rice crop

shows significant temporal behaviour and a large dynamic range (-14.4 to -8.41dB) during its growth period(Fig. 4).

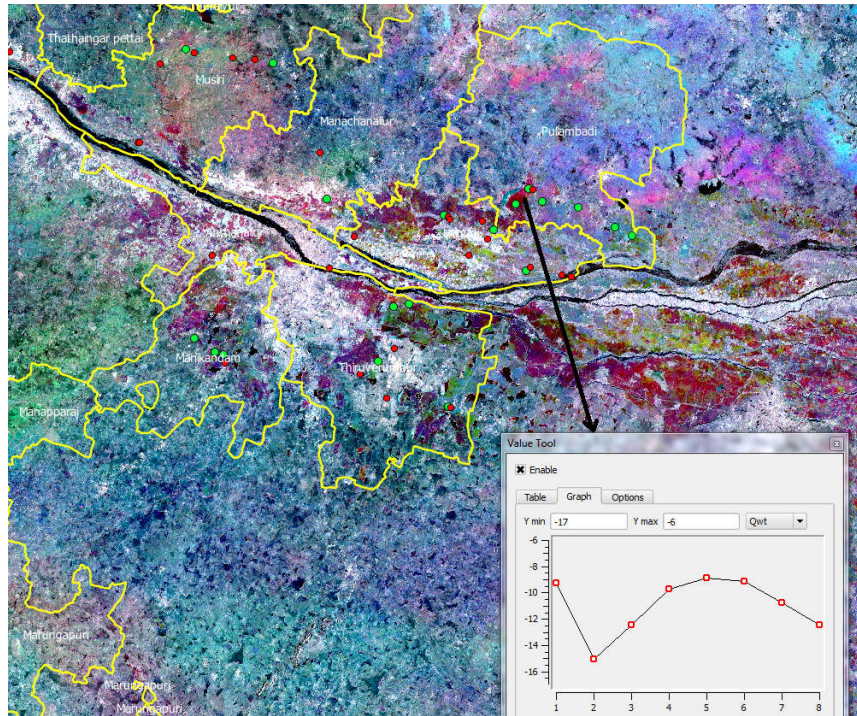


**Fig.1. dB stack generated with Sentinel 1A data and Rice Temporal Signature**

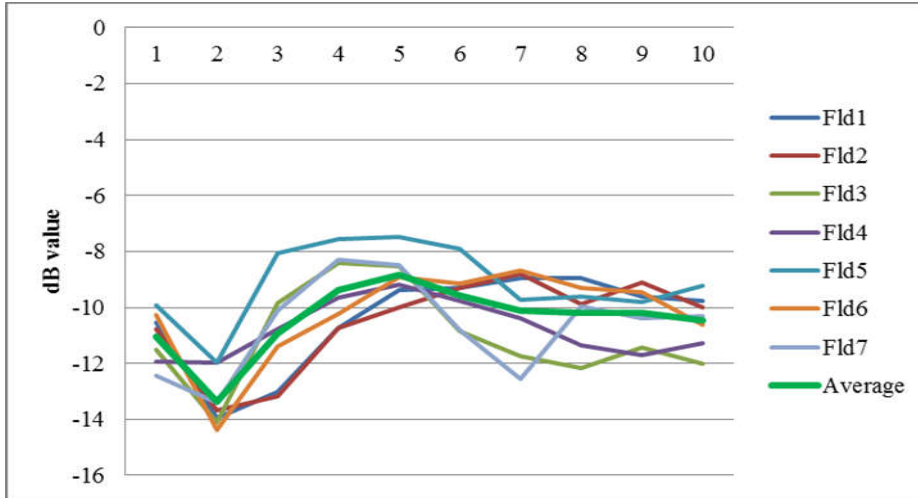


**Fig.2. dB curves for rice at Monitoring sites**

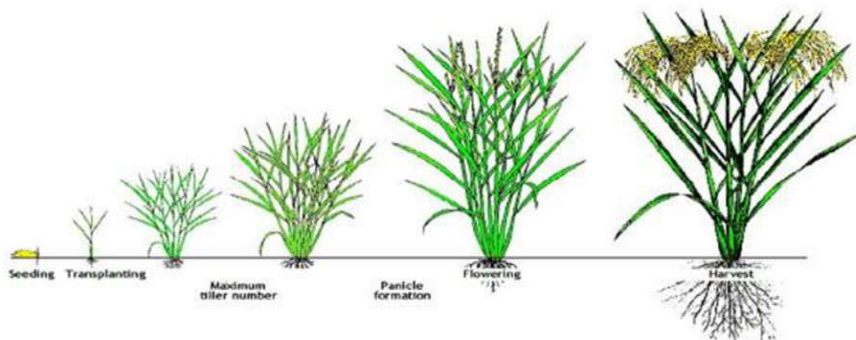


**Fig.3. Rice crop stages (Image from the International Rice Research Institute (IRRI)-Rice Knowledge Bank.)**

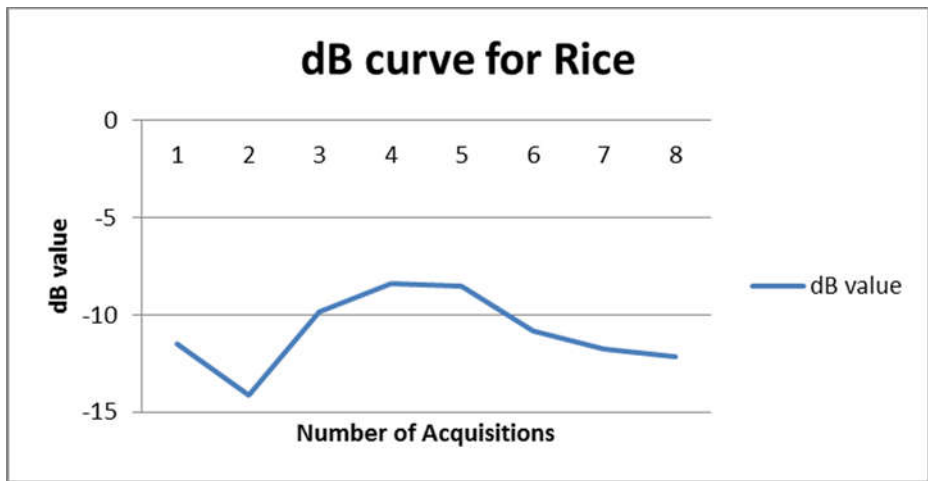


Fig.4. Temporal dB curve for rice crop Sentinel 1A data

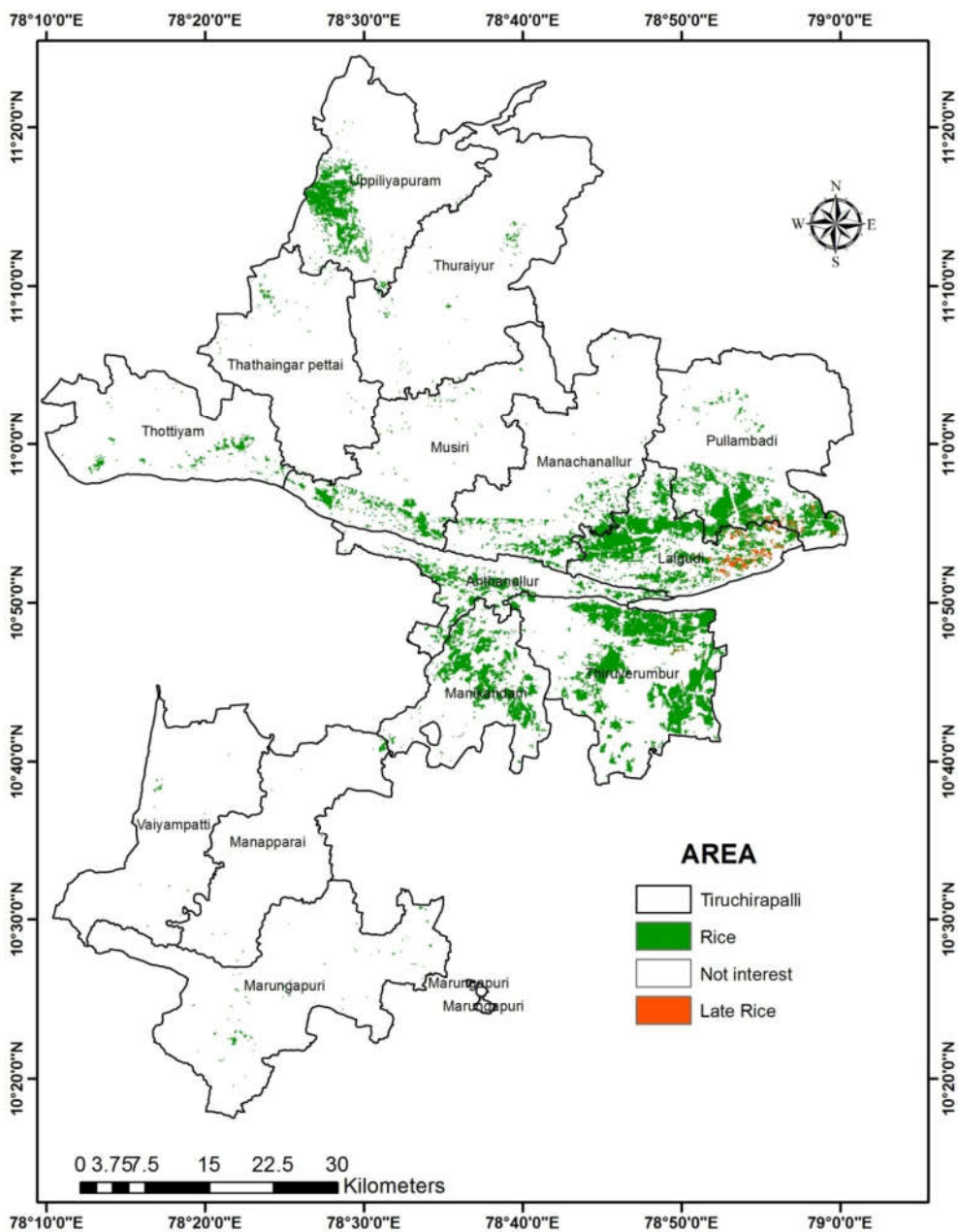


Fig.5. Rice area map of Tiruchirapalli District

**Table.1. Temporal dB values of rice fields across Tiruchirapalli district**

Satellite pass no.	Field 1	Field 2	Field 3	Field 4	Field 5	Field 6	Field 7	Average
1	-10.5271	-10.7566	-11.5084	-11.9302	-9.91686	-10.2864	-12.4375	-11.0518
2	-13.9591	-13.6708	-14.1164	-11.99	-11.9655	-14.3656	-13.4124	-13.3542
3	-13.0355	-13.1874	-9.83019	-10.788	-8.05275	-11.3981	-10.1088	-10.9144
4	-10.7231	-10.7202	-8.41801	-9.65563	-7.55453	-10.2313	-8.27749	-9.36861
5	-9.38419	-9.99612	-8.52289	-9.17506	-7.49632	-8.89452	-8.48584	-8.8507
6	-9.30455	-9.29256	-10.8482	-9.75389	-7.89242	-9.14254	-10.799	-9.57617
7	-8.94641	-8.78155	-11.753	-10.3778	-9.7139	-8.67064	-12.5686	-10.116
8	-8.95322	-9.87542	-12.1777	-11.3539	-9.61987	-9.31618	-9.94272	-10.177
9	-9.59416	-9.11129	-11.4259	-11.6926	-9.7905	-9.45091	-10.4037	-10.2099
10	-9.76227	-10.0025	-11.999	-11.283	-9.20801	-10.6254	-10.3029	-10.4547

**Table.2. Temporal dB value for rice crop from Sentinel 1A data**

Sl.No.	Date of acquisition	dB value
1	01-Sep	-11.5084
2	19-Oct	-14.1164
3	31-Oct	-9.83019
4	12-Nov	-8.41801
5	24-Nov	-8.52289
6	06-Dec	-10.8482
7	18-Dec	-11.753
8	30-Dec	-12.1777

### ***Spatial assessment of Rice area***

Rice in tropical and subtropical Asia is mainly cultivated in irrigated or lowland rainfed conditions. Rice varieties range in duration from 90 to more than 150 days and with three main crop stages: vegetative (from germination to panicle initiation, from 45 to 100 days), reproductive (from panicle initiation to flowering, around 35 days) and maturity (from flowering to mature grain, around 30 days) (Fig. 3). The following aspects contribute to the change in space occupied by the rice plants within a three-dimensional space: (1) appearances and growth of leaves from the main stem (culm) and tillers; (2) stem development and elongation; (3) tillering, defined as the production of stems from rice plants; (4) leaf senescence; and (5) panicle and grain development. New Rice leaves appear approximately every four days during the vegetative phase and every seven days during the reproductive phase. Tillering begins at around the three- to four-leaf stage or approximately 10 days after emergence.

Research effort was taken to use multi-temporal C-band SAR data from Sentinel 1A, semi-automated processing chains, in-season field monitoring and end-of-season validation points to map rice crops across Tiruchirapalli District. SAR data have a proven ability to detect lowland rice systems (both irrigated and rainfed) through the unique temporal signature of the backscatter coefficient (also termed sigma naught -  $\sigma^0$ ) exhibited by the crop. In the past years, lot of research efforts were taken for better understanding this relationship and applying it to rice detection and rice monitoring.

Temporal signatures were extracted for each monitoring field and used to generate the dB curves for rice fields. Fig.2 shows the temporal signature for selected representative pixels to visualize the resulting rule based classification. Rice crop shows significant temporal behaviour and a large dynamic range (-14.4 to -8.41dB) during its growth period. This is due to the interaction of microwave radiation with the crop canopy, increasing from the detection of  $\sigma^0$  minimum (field inundation) to the detection of  $\sigma^0$  maximum

(around the tillering stage) between acquisitions four and six. In the case of “early rice,” the SAR series did not capture the  $\sigma^{\circ}$  minimum, since it occurred before the first acquisition; however, an increase in backscatter is observed during the growth period for the first four acquisitions that is typical of the seedling to tillering stage. In the case of “late rice,” the first four SAR acquisitions show a high backscatter value because, during that period, the fields were in fallow condition (as confirmed in the ground observations). The backscatter minimum was observed in the sixth acquisition, indicating flooded conditions, followed by an increase in backscatter in the succeeding acquisitions, indicating growth of the rice crop. The other field crop signal showed a distinctly different temporal evolution and the absence of any evidence of a water signal at the start of crop growth which helped precise discrimination of rice crop pixel by pixel. In short, this temporal variation of SAR backscatter differentiates rice fields from other land cover classes.

Rice area map was derived from multi-temporal C-band SAR imagery from Sentinel 1A for all the 14 blocks of Tiruchirapalli district. Late rice and early rice were combined into one class and they were distinguished from rice in the maps below for discussion purposes. Map accuracy considers any of the three rice subclasses as rice. The overall classification accuracy was consistently high (92.0 %), with Kappa score of 0.84. In total 50 validation points covering 21 rice and 29 non-rice points were collected for accuracy assessment. Since the rice area in the district was in less proportion to non rice area, more non-rice points were used for accuracy assessment. The SAR data was able to detect rice points precisely and the automated algorithms were capable of discriminating rice pixels from pixels of other crops.

The consistently high accuracy of the rice area classification across these blocks demonstrated that the methodology was appropriate for rice detection across the most common rice agro-ecologies. The classification was based on a temporal analysis of the spectral signature, including a detection of agronomic flooding at the land preparation and/or seedling stage followed by a rapid increase in biomass relative to the duration of the vegetative stage of the varieties in the sensor footprint. The monitoring site data were critical for the correct interpretation of the spectral signature.

## CONCLUSION

Spectral dB curve rice was generated using temporal multirate Sentinel 1A data. A detailed analysis of temporal signatures of rice showed a minimum at agronomic flooding and a peak at maximum tillering stage and decreasing thereafter. Rice crop expressed a significant temporal behaviour and a large dynamic range (-14.4 to -8.41 dB) during its growth period. At flooding, minimum dB value from -14.36 to -11.992 was recorded with an average of -13.35. The average maximum value at peak at tillering stage was found to be -8.85 dB in fields across Tiruchirapalli district with a primary variation of 1.5 to 2.1 dB and a secondary variation of 2.5 to 3.5 dB corresponding to growth at vegetative and maximum tillering stage. Rice area map was generated using a rule based classifier approach with a classification accuracy of 92.0 per cent and Kappa score of 0.84.

## ACKNOWLEDGEMENT

Author very thankful to <sup>1</sup>Department of Remote Sensing and GIS, Tamil Nadu Agricultural University, Coimbatore – 641003 provide all the necessary inputs/information to complete this work.

## REFERENCES

1. Aspert, F., M. Bach Cuadra, A. Cantone, F. olecz, J. P. Thiran. (2007). Time-varying segmentation for mapping of land cover changes. In: Proceedings of ENVISAT Symposium, Montreux, Switzerland. 23-27.
2. Boschetti, M., F. Nutini, G. Manfron, P.A. Brivio and A. Nelson. (2014). Comparative analysis of normalised difference spectral indices derived from MODIS for detecting surface water in flooded rice cropping systems. *PLoS One*, 9: 88741.
3. Bouvet, A., T. le Toan and Lam-Dao. (2009). Monitoring of the rice cropping system in the Mekong delta using ENVISAT/ASAR dual polarization data. *IEEE Trans. Geosci. Remote Sens.*, 47:517-526.
4. De Grandi, G.F., M. Leysen and J.S. Lee, D. Schuler. (1997). Radar reflectivity estimation using multiple SAR scenes of the same target: Technique and applications. In: Proceedings of the IEEE. International Geoscience and Remote Sensing “Remote Sensing-A Scientific Vision for Sustainable Development” (IGARSS '97), Singapore, 3-8 August. pp. 1047-1050.
5. Gumma, M.K., P.S. Thenkabail, A. Maunahan, S. Islam and Nelson. (2014). A Mapping seasonal rice cropland extent and area in the high cropping intensity environment of Bangladesh using MODIS 500 m data for the year. *ISPRS J. Photogramm. Remote Sens.*, 91: 98-113.
6. Holecz, F., M.F.L. Barbieri, A. Collivignarelli, T.D.M. Gatti, Nelson, G. Setiyono, Boschetti, P.A.B. Manfron, J.E. Quilang. (2013). An operational remote sensing based service for rice production estimation at national scale. In: Proceedings of the Living Planet Symposium, Edinburgh, UK, 9-11.
7. Huke, R.E and E.H. Huke. (1997). Rice area by type of culture: South, Southeast, and East Asia. A revised and updated data base'. International Rice Research Institute: Manila Philippines.

8. Inoue, Y. E. and Sakaiya. (2013). Relationship between X-band backscattering coefficients from high- resolution satellite SAR and biophysical variables in paddy rice. *Remote Sens. Lett.* 4: 288–295.
9. Inoue, Y. T. Kurosu, H. Maeno, S. Uratsuka, T. Kozu, K. Dabrowska-Zielinska, J. Qi. (2002). Season - long daily measurements of multifrequency (Ka, Ku, X, C, and L) and fullpolarization backscatter signatures over paddy rice field and their relationship with biological variables. *Remote Sens. Environ.*, 81: 194–204.
10. Inoue, Y., E. Sakaiya, C. Wang. (2014). Capability of C-band backscattering coefficients from high-resolution satellite SAR sensors to assess biophysical variables in paddy rice. *Remote Sens. Environ.*, 140: 257–266.
11. Le Toan, T, F. Ribbes, L.F. Wang, N. Floury, K.H. Ding, J.A. Kong, M. Fujita and T. Kurosu. (1997). Rice crop mapping and monitoring using ERS-1 data based on experiment and modeling results. *IEEE Trans. Geosci. Remote Sens.*, 35: 41–56.
12. Lopez-Sanchez, J.M., J.D. Ballester-Berman, I. Hajnsek. (2011). First results of rice monitoring practices in Spain by means of time series of Terra SAR-X dual-pol images. *IEEE J. Sel. Top. Appl. Earth Obs. Remote Sens.*, 4: 412–422.
13. Lopez-Sanchez, J.M., S.R. Cloude, J.D. Ballester-Berman. (2012). Rice phenology monitoring by means of SAR polarimetry at X-band. *IEEE Trans. Geosci. Remote Sens.*, 50: 2695– 2709.
14. Maclean, J.L., B. Hardy, G.P. Hettel. 2013. *Rice Almanac*. 4<sup>th</sup> ed. International Rice Research Institute: Los Banos, Philippines, p. 298.
15. Nelson, A., Setiyono, T., Rala, A. B., Quicho, E. D., Raviz, J. V, Villano, L. S., ... Detoito, N. T. (2014). Towards an Operational SAR-Based Rice Monitoring System in Asia: Examples from 13 Demonstration Sites across Asia in the RIICE Project, 10773–10812. <http://doi.org/10.3390/rs61110773>
16. Nguyen, T.T.H., C.A.J.M. de Bie, A. Ali, E.M.A Smaling, T.H. Chu. (2012). Mapping the irrigated rice cropping patterns of the Mekong delta, Vietnam, through hyper-temporal SPOT NDVI image analysis. *Int. J. Remote Sens.*, 33, 415–434.
17. Oh, Y, S.Y., Hong, Y. Kim, J.Y. Hong and Y.H. Kim. (2009). Polarimetric backscattering coefficients of flooded rice fields at L- and C-bands: Measurements, modeling, and data analysis. *IEEE Trans. Geosci. Remote Sens.*, 47, 2714–2721.
18. Pazhanivelan, S., P. Kannana, P. Christy Nirmala Marya, E.Subramaniana, S. Jeyaraman, Andrew Nelson , Tri setiyono, Francesco Holecz, Massimo barbieri and ManojYadav. (2015). Rice Crop Monitoring and Yield estimation through Cosmo Skymed and Terrasar-X: A SAR-Based Experience In India. 2015. The 36<sup>th</sup> International Symposium on Remote Sensing of Environment, 11 – 15 May, Berlin, Germany, ISRSE36-711-1.
19. Suga, Y and T. Konishi, (2008). Rice crop monitoring using X-, C- and L band SAR data. *Proc. SPIE*, 7104, 710410.

#### CITATION OF THIS ARTICLE

N.S. Sudarmanian and S. Pazhanivelan. Detection of SAR Signature for Rice Crop using SENTINEL 1A data *Bull. Env. Pharmacol. Life Sci.*, Vol 8 [7] June 2019: 32-39